Gasdynamics of the Cryogenic Cooler of the Nimbus F Spacecraft

William J. Rae* and Michael G. Dunn*
Calspan Corporation, Buffalo, N. Y.

This paper presents a theoretical study of the gasdynamic behavior of the system used to vent methane gas from an open-cycle cryogenic cooler carried on the NIMBUS F satellite. The flow of this gas from the cryogen tank to the vent-line exit takes place at very low Reynolds number, and is strongly affected by variations in the tube cross-sectional area, substantial heat addition, and important frictional effects. All three of these factors play a role in determining the choking mass flow. Finite-difference calculations are used to establish the mass flow rates for a range of cryogen temperatures. Finite-difference calculations are also used to determine the flowfield in the plume that results when the vented gas exits from the spacecraft. The momentum-flux distributions within the plume are then used to estimate the torques applied to the spacecraft when the plume impinges on several surfaces near the exit point. These torque estimates compare favorably with flight data.

Nomenclature

C_D = discharge coefficient
C_p, C_v = specific heat at constant pressure, volume
D = pipe diameter
f = friction coefficient
F = thrust
$\dot{m}$ = mass flow rate
p = pressure
R = pipe radius
T = temperature
t = time
u = axial component of velocity in pipe
u_n = velocity component in plume, normal to spacecraft surface
V_e = velocity at pipe exit plane
γ = specific heat ratio
μ = viscosity
ρ = density

Introduction

THE Nimbus F spacecraft experienced a torque when methane gas from an open-cycle cryogenic cooler (used on the LRIR† experiment) was vented in orbit. Two possible explanations for the observed torque are a) the methane vent pipe may have been misaligned with the spacecraft center of gravity resulting in a thrust-induced torque, or b) the vented gas may have impinged on nearby surfaces of the spacecraft resulting in nonsymmetric torques.

The purpose of this paper is to describe a theoretical study of the gasdynamic motion of the vent gas from the methane cooler through the tubing to the exit plane, concluding with a plume calculation to determine potential impingement surfaces and exhaust thrust levels. The mass flow rates of methane as a function of cryogen temperature are an important part of these calculations and are described in detail. The results of the calculations identify plume impingement as the probable cause of the torques; the calculated results compare favorably with flight data.

Received April 30, 1976; revision received Oct. 7, 1976. This work was sponsored by NASA Langley Research Center, Hampton, Va. A more extensive discussion of this work can be found in NASA CR 145045. The authors are indebted to N.D. Akey and J.J. Scialdone for many valuable discussions of this problem.

Index categories: Boundary Layers and Convective Heat Transfer–Laminar; Spacecraft Attitude Dynamics and Control.

*Principal Engineer, Aeordynamic Research Department. Member AIAA.

†Limb Radiance Inversion Radiometer.

Physical Configuration of Cryogenic Cooler and Nimbus F Spacecraft

Figures 1 and 2 illustrate the physical configuration of the cryogenic cooler and the associated plumbing as well as the thermal environment of the overall system which must be included in the analysis of the gasdynamics problem. Methane flow initiates in a corrugated tube with an effective inside diameter of approximately 0.843 cm (0.33 in.) and remains at a wall temperature corresponding to the solid methane temperature for a distance of approximately 35.56 cm (14 in.). At this point, the tube passes through a short insulation section and then through the ammonia tank for a distance of approximately 21.59 cm (8.5 in.). The tube wall temperature in passing through the ammonia tank is on the order of 140 to 150 K. Shortly after exiting from the ammonia tank, the 0.843-cm diameter line becomes a 2.54-cm diameter line which then goes for a distance of approximately 91.44 cm at which point an explosively-actuated squib valve is located. The temperature of the 2.54-cm diameter tube is approximately 280 K. The inside diameter of the squib is 1.27 cm and its length is on the order of 2.54 cm. Downstream of the squib there is an additional 20.32 cm of 2.54-cm diameter line (also at 280 K) at the end of which the methane exhausts to the environment.

The tendency of this wall-temperature distribution is to add energy to the flow, which causes a velocity increase and a thicker boundary layer, and drives the flow toward a thermally choked condition. The frictional resistance caused by boundary-layer growth drives the flow toward viscous choking, and both of these effects interact with the inviscid mechanisms generated by variations in the cross-sectional area. Figure 3 is a sketch‡ of the Nimbus F-LRIR configuration. It is apparent from this sketch that surfaces 1, 2, and 3 were potential impingement surfaces.

The local gas density, flow velocity, and flow angle were calculated at selected points in the plume and these results were used to calculate the impingement forces. The flow conditions at the exit plane of the vent pipe were used as input conditions for the plume calculation. Since the relative location of the spacecraft c.g. is known, the resultant torques about each of the axes can be estimated.

‡The detailed drawings from which this sketch was made were supplied to us by J. Keough, General Electric Company, Philadelphia, Pa.

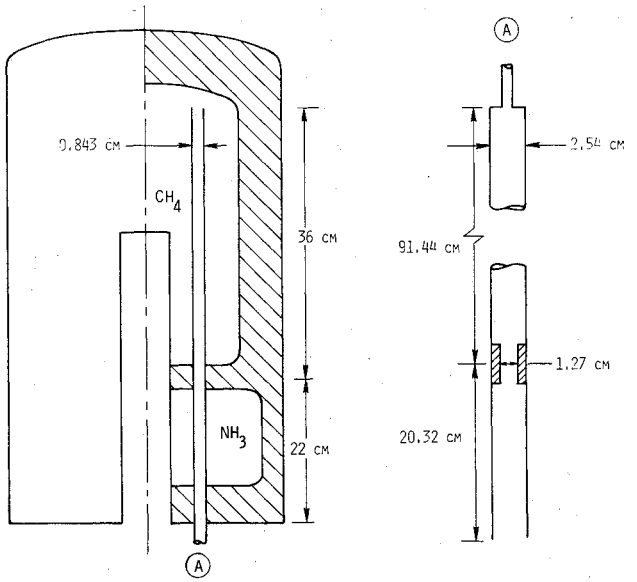

Fig. 1 Physical configuration of cooler and associated plumbing.

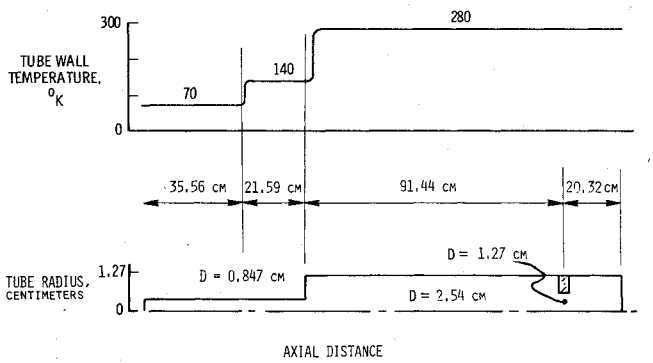

Fig. 2 Representation of tube wall geometry and temperature conditions.

Basic Approach to Solution of Problem

Flow in Internal Pipes

The flow in the tubing leading to the venting exit plane was calculated using a computer program developed some years ago for predicting flow phenomena in low-thrust rockets.[1,2] The predictive capability of this program has been demonstrated experimentally.[3,4]

The calculation method is based on the slender-channel equations, which are essentially the Navier-Stokes equations simplified for flows in large length-to-diameter channels. The solution is found by a finite-difference method, using a Crank-Nicholson implicit scheme. Thus, the complete flowfield is found, including the full effects of two-dimensionality, compressibility, friction, and heat transfer. No a priori assumptions about the skin-friction or heat-transfer coefficients need to be made; they are calculated as a part of the solution

The calculations require only a description of the pipe geometry, the distribution of wall temperatures along the pipe, and the properties of the gas (such as its specific-heat ratio, Prandtl number, and viscosity). The solution is then found for a series of mass flow rates; by examining these solutions, it is possible to determine the maximum flow rate that the gasdynamic constraints will allow, before the limits imposed by thermal and/or frictional choking are reached.

Description of External Plume

The methane plume was calculated using a vacuum-plume predictive code.[5] For the current application, conditions at the exit plane of the pipe are calculated using the method previously described. These results form the input conditions to the program which then calculates the gasdynamics of the plume gases as they expand into the ambient environment.

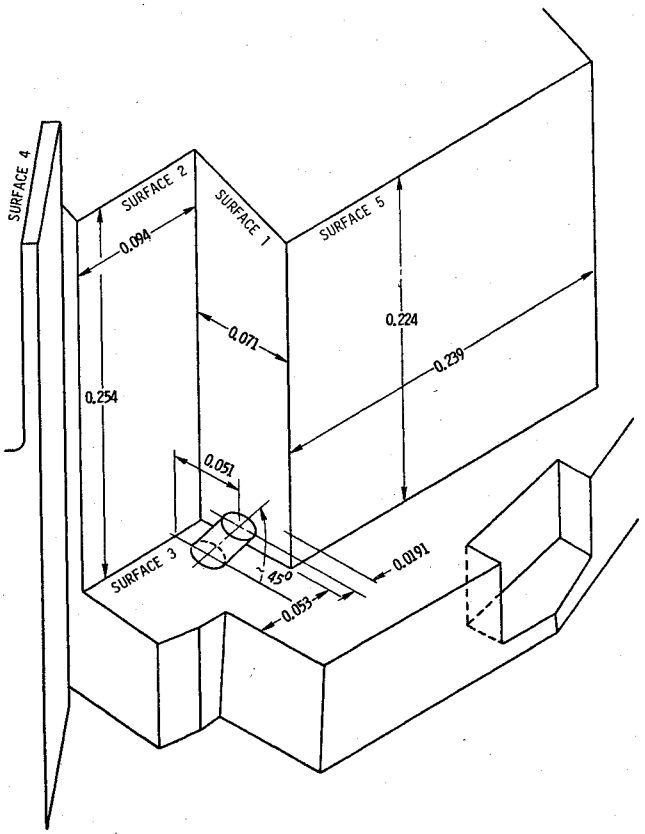

Fig. 3 LRIR configuration (all dimensions in meters).

Discussion of Results

Representation of the Vent Line

For the purpose of defining the gasdynamic behavior of the tubing, the two most significant features are the distributions of wall temperature and cross-sectional area. These distributions were represented in the manner shown in Fig. 2. The transitions between the various temperatures levels were modeled by a cosine function, whose length was shorter than the insulation thickness; more accurate representation of these transitions could have been made, based on estimates of the temperature distribution within the insulation layers, but were not felt to be warranted. One check calculation was done with 5.08 cm thickness for these transitions, at a methane temperature of 70 K. The results were essentially unchanged.

The area-ratio distribution is perhaps the most significant feature of the system. In attempting to predict the mass flow into a near-vacuum environment, one instinctively looks for sonic choking at the section of minimum cross-sectional area. For the present system, that occurs in the 0.847-cm diameter line, a section where significant heat transfer would be exptected. Thus, the possibility of thermal choking needed to be evaluated. In addition, the small diameter and low vapor pressures involved make this very low Reynolds number flow, with the attendant possibility of thick laminar boundary layers and frictional choking.

Method of Analysis

It is relatively easy to analyze flows of this type by means of a one-dimensional approximation, in which the effects of friction and heat transfer are estimated by guessed values of the transfer coefficients. However, the results are critically dependent on the values assumed. For the present calculations, a finite-difference calculation of the flow was made, which

required no approximations beyond those implicit in the use of the Navier-Stokes equations.

The methane was taken to be a perfect gas, with constant specific heats, whose ratio $\gamma = C_p/C_V$ was taken as 1.31, Prandtl number equal to 0.772, and with a viscosity-temperature law of the form

$$\mu/\mu_0 = (T/T_0)^{1.0}$$

with $\mu_0 = 2.75 \times 10^{-6}$ kg/m-sec at $T_0 = 70$ K.§ Unit accommodation coefficients were used in the first-order slip boundary conditions applied at the tube walls.[1]

Solutions in the 0.847 cm Line for Solid Methane Temperature 70 K

The computer program described in Ref. 2 was modified slightly, in order to handle flow in a constant-area channel. For each of several values of the methane temperature, the flow was calculated for a series of mass flow rates. Figure 4 shows a typical set of results for a methane temperature of 70 K. In flowing through the methane-tank section, the wall and stagnation temperatures are the same, and so essentially no heat transfer occurs. The shear stress at the walls causes a frictional pressure drop, which is accurately represented (as long as the Mach number does not approach 1.0) by the Hagen-Poiseuille law[6]

$$dp/dx = -8\mu_0 \dot{m}/\pi\rho_0 R^4$$

where the subscript zero denotes conditions at rest in the methane tank, and R is the tube radius.

The wall temperature in the ammonia-tank section of the line was taken to be 140 K (except for one calculation, discussed below, in which it was raised to 159 K) based on the flight data which indicate values from around 140 K to 153 K. Upon entering this section of the line, a very substantial heat transfer to the gas takes place. The elevated temperature of the gas, in layers near the wall, causes a proportionate decrease in density, and a consequent acceleration of the flow, in order to maintain the same mass flow. This increased acceleration and attendant increase in wall shear is balanced by a steeper negative pressure gradient, and the net effect of the heat-transfer process is to drive the subsonic flow toward Mach one. This process leads to the condition known as thermal choking; i.e., the acceleration continues until a small region near the centerline actually becomes slightly supersonic. When it does, the decreasing pressure causes the streamlines in this region to expand, thus crowding the subsonic layers nearer to the wall. These layers, in turn, respond to the decreasing area allowed them by further increasing their acceleration toward the sonic condition, and the whole process quickly arrives at a condition where the flow cannot continue without some increase in the cross-sectional area. If this occurs upstream of the transition to the 2.54-cm diameter line, pressure waves originating at the choked station will quickly propagate back into the methane tank, causing a decrease in the flow rate.

These pressure waves are not calculated in the computer program, which assumes a steady flow. Instead, when the calculation detects a choked condition in the 0.847-cm diameter line, the calculation must be restarted at the tube entrance, with a reduced value of the mass flow. This sequence is continued until a solution is found for which the choking condition occurs just at the end of the 0.847 cm section. For a methane temperature of 70 K, this condition was reached for a mass flow rate of 2.26×10^{-5} kg/sec, as shown in Fig. 4.

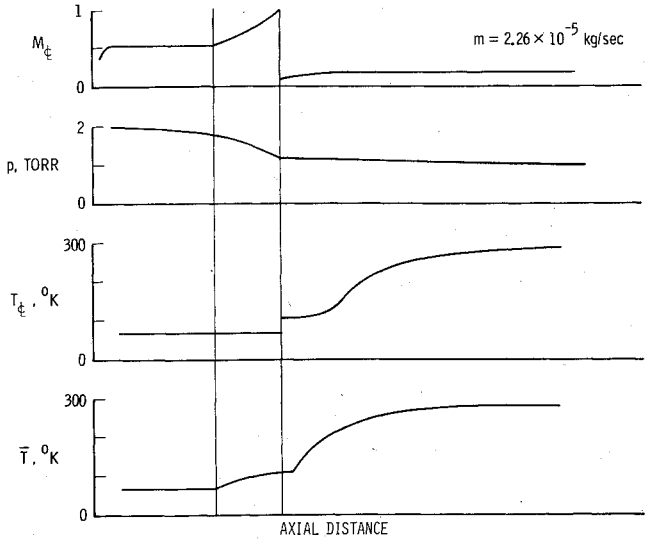

Fig. 4 Gasdynamic results for methane temperature of 70 K.

Solution in the 2.54 cm Line

Upon leaving the ammonia-tank portion of the line, the thermally choked flow encounters a 9-to-1 increase in cross-sectional area, and a doubling of the wall temperature. These conditions operate in opposing directions: the increase in area tends to accelerate the flow toward supersonic conditions, while the heat addition tends to drive the Mach number toward one. For the case shown in Fig. 4, the average temperature of the methane, defined as

$$\bar{T} = \frac{\int_0^R \rho u (C_p T + \tfrac{1}{2}u^2) \cdot 2\pi r dr}{C_p \int_0^R \rho u \cdot 2\pi r dr}$$

has not yet reached the wall temperature of 140 K at the end of the 0.847 line. Thus, the prospective effect of heat addition in the 2.54 cm line is roughly a tripling of the stagnation enthalpy of the flow.

One approach to the resolution of these competing tendencies would be to attempt the continuation of the finite-difference calculations into the one inch line. To do so would require an effective wall shape to model the recirculation zone occurring at the transition in tube diameter. If a suitable location of the dividing streamline and a suitable representation of the heat transfer in the vicinity of the recirculation zone could be found, the finite-difference calculations could be carried into the 2.54 cm line. This route was not followed, however, because there is clear evidence that it would only reveal an eventual breakdown of supersonic flow, signifying that the flow in the 2.54 cm line follows a subsonic branch, which is more easily calculated by a method outlined below.

The evidence against the possibility of supersonic flow in the one inch line comes from a one-dimensional analysis.[7] In the absence of friction and heat transfer, the 9-to-1 area ratio would accelerate the flow from the sonic condition to a Mach number of 3.5.[8] This supersonic flow, however, can only sustain a stagnation-temperature rise by a factor of 1.79 before it returns to Mach number one. For the conditions of the present calculations, the impressed temperature change in the 2.54 cm section is larger than this value.

In addition to this evidence, the area contraction at the squib also rules out the possibility of supersonic flow in the 2.54 cm pipe. Even in the absence of friction and heat transfer, it is well known from the field of supersonic diffuser design[7] that a Mach 3.5 flow cannot be recompressed through a 4 to 1 area contraction. Such a device would not start, i.e.,

§Private communication with Dr. R Boericke, General Electric Company, Philadelphia, Pa. Viscosity based on Lennard-Jones potential with $\sigma = 3.822$ Å and $\epsilon/K = 137$ K.

pressure waves would quickly travel upstream from the contraction, returning the flow to the subsonic branch.

Thus, it can be concluded that the flow in the 2.54 cm section follows the subsonic branch; for this case, the 9-to-1 area ratio drops the Mach number to around 0.07. This flow can sustain a stagnation temperature rise by a factor of around 50 before choking.

Since the Mach number drops to such a small value, the flow can be adequately handled by assuming that it starts, immediately downstream of the area change, as a new Poiseuille flow, with a parabolic velocity profile, and with a uniform temperature profile, equal to the mean stagnation temperature at the end of the 0.847 cm section. In reality, there will be a short mixing region at the beginning of the 2.54 cm section; the approximation made here neglects this additional length.

Passage through the Squib

For the case where the solid methane temperature is 70 K, the calculation of the subsonic pipe flow in the 2.54 cm line (for $\dot{m} = 2.26 \times 10^{-5}$ kg/sec, the value determined by thermal choking at the end of the 0.847 cm section) can be carried up to the location of the squib. In this section of the pipe, there is a slight pressure drop, and the residence time is sufficiently long that the flow uniformly acquires the wall temperature, with only a modest increase in Mach number. The next question that arises is, can this flow pass through the area constriction at the squib without further gasdynamic complications?

To answer this question, it is necessary to review what normally takes place when a low Reynolds number flow starts from rest at a given pressure and temperature, and passes through a geometric throat[1]: if the pressure into which the nozzle is exhausting is negligible compared to the stagnation pressure upstream of the throat, there will be a unique mass flow that will produce choking conditions at the throat. In general, this flow will have a Mach number equal to one on the centerline, and will have fairly thick boundary layers, i.e., the mass flow will be somewhat less than the ideal value.

For the present situation, however, these considerations are insufficient, since the mass flow has already been determined by the condition of thermal choking upstream. Thus, the problem is that of two throats operating in series, with the second throat capable of passing a higher mass flow than the first. As in other instances, the mass flow is set by conditions at the first throat, and this mass flow is matched to conditions at the second throat by a stationary system of compression or expansion waves.¶ For the present case, this matching could easily be achieved by a fairly weak compression-wave system near the start of the 2.54 cm line; the flow would undergo an expansion to slightly supersonic conditions, and would then pass through a compression-wave system that would raise its pressure slightly, before mixing and slowing down. The flow from this station to the squib is then essentially the same as that described earlier, except that the static pressure has now been adjusted to the level required to match the discharge coefficient of the squib. This process is illustrated in Fig. 5 by the crossing of two curves: the first of these, with a positive slope, shows the discharge coefficient for a flow that starts from a very low Mach number, at a temperature of 280 K, and a given static p, and accelerates to a choked condition in the squib. As the pressure rises, the boundary layer becomes thinner, and the discharge coefficient goes up. The second curve, with a steep negative slope, shows what the discharge coefficient must be for a given mass flow, and various values of p, i.e., as p increases, the ideal mass flow increases in direct proportion, and so the discharge coefficient corresponding to a given mass flow will vary inversely as p. For the case shown, this curve has the value $C_D = 0.761/p$, where p is measured in torr.

The conclusion, for the present case, is that the mass flow can be matched to the second throat by any loss mechanism that will fix the pressure upstream of the squib at a value around 0.87 torr.

¶The authors are grateful to R. C. Weatherston of the Aerodynamic Research Department, Calspan Corporation, for an enlightening discussion of this subject, and to one of the reviewers for noting the condition that the second throat must be capable of passing a higher mass flow than the first.

Flow Downstream of the Squib

The flow through the final 20.32 cm downstream of the squib is governed by the competing effects of friction and area change; there is essentially no further heat addition.

Because this flow is exhausting into a near vacuum, the 4-to-1 area increase downstream of the squib tends to accelerate the flow to supersonic conditions. In the absence of friction, a one-dimensional estimate would place the Mach number at a value of about 2.75. However, this low-density supersonic flow must then overcome the effects of friction, over eight more diameters. It is easy to estimate whether this can be done, by using the one-dimensional results for flow with friction in a constant-area channel.[7] These results show that for a given initial Mach number and a given friction coefficient f (defined as $f \equiv 2\tau_w/\bar{\rho}\bar{q}^2$, where τ_w is the wall shear stress, $\bar{\rho}$ the mean density, and $\bar{q}^2$ the mean square of the velocity profile) there is a maximum duct length L_{max} that will lead to frictional choking. If the duct is longer then some other mechanism will intervene.

A reasonable estimate of the friction factor is the laminar value

$$f = 16\pi\mu R/\dot{m}$$

If μ is evaluated at the wall temperature (280 K), this gives (for $R = 1.27$ cm)

$$f = 6.70 \times 10^{-6}/\dot{m} \qquad [\text{kg/sec}]$$

Thus, for the 70 K case, the value of $4fL/D$ is 9.5. For an initial Mach number of 2.75, however, the maximum value, corresponding to frictional choking,[8] is $4fL_{max}/D = 0.58$. Thus, according to the discussion given by Shapiro,[7] it can be expected that a compression-wave system will intervene, reducing the Mach number just downstream of the squib to a subsonic value such that the flow can subsequently accelerate to sonic conditions again at the exit plane. This distribution of Mach number downstream of the squib has not been calculated explicitly by the finite-difference program, and consequently is not shown in Fig. 4. It is sufficient for purposes of the later plume calculation to know that sonic conditions exist at the exit plane.

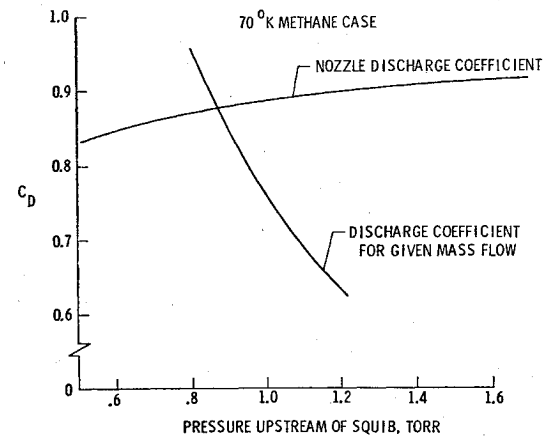

Fig. 5 Matching of the discharge coefficient for flow through the squib.

Summarizing the flow behavior for the case where the solid methane temperature is 70 K: the mass flow is determined by the condition of thermal choking, at the end of the 0.847 cm line, due to heat extraction from the solid ammonia. Upon entering the 2.54 cm line, this flow is unable to expand to supersonic conditions, and makes its way to the squib location, where it accelerates to sonic flow. The matching of this critical flow rate to the value dictated by thermal choking is achieved by a pressure-adjustment mechanism in the 2.54 cm line, upstream of the squib. After passing through the squib, the flow accelerates briefly, and then encounters another compression-wave system which reduces its Mach number to a subsonic value, sufficiently low so as to allow negotiation of the frictional resistance in the final 20.32 cm. The flow emerges at the exit plane in a condition of frictional choking, i.e., the Mach number is very close to one. Because of the long residence time in the one inch line, the temperature can be assumed to be equal to the wall temperature, here taken as 280 K.

Solution for Other Solid Methane Temperatures

The sequence of calculations described above was repeated, for solid methane temperatures of 85 K, 75 K, and 65 K. Results for the two higher temperatures reveal no new phenomena other than those already encountered at 70 K. The mass flows from these cases are summarized in Fig. 6. The data in Fig. 6 also show one calculation, done at 85 K, for which the ammonia temperature was taken as 159 K. The mass flow under these conditions is essentially the same as for 140 K.

However, the results for 65 K reveal that the mechanism of frictional choking in the one-inch diameter line takes over as the feature controlling the mass flow. This can be seen by examining curve 2 in Fig. 7, which shows the solution for the mass flow which chokes thermally at the end of the 0.847 cm line. When this solution is continued into the 2.54 cm line, it chokes due to friction, well upstream of the squib. The solution for a lower mass flow, labeled curve 1 in Fig. 7, is able to reach the squib location without choking. In order to make a precise determination of the mass flow for this case, it would be necessary to pursue these calculations further, including the region downstream of the squib. The final mass flow would be that one for which frictional choking occurs at the exit plane. For purposes of the present investigation, these calculations were not warranted, since they involve the very difficult problems of guessing an approximate stream-surface geometry on passing through the squib, and because the actual flow may involve pressure-adjustment mechanisms that are not included in the computer-program formulation. Consequently, it was decided to use the two solutions of Fig. 7 as an upper and lower bound for the mass flow at 65 K, and these are shown in Fig. 6.

The summary of mass flow rates as a function of methane temperature, shown in Fig. 6, carries an indication that the frictional choking mechanism becomes the dominant one somewhere between 65 K and 70 K, but it should be understood that the location of this boundary has not been precisely defined.

The fact that frictional choking in the 2.54 cm line becomes the dominant mechanism at 65 K is also indicated by a one-dimensional analysis,** in the following way: in the discussion of the 70 K case, given above, it was argued that a compression wave appears in the flow downstream of the squib, and that this system would reduce the Mach number to a subsonic value low enough to allow a subsequent acceleration back to Mach one at the exit plane. Table 1 below shows what the initial Mach number must be for $L/D=8$, using the laminar friction factor defined earlier.

**The authors are very grateful to R. Boericke of the General Electric Company for pointing out this mechanism.

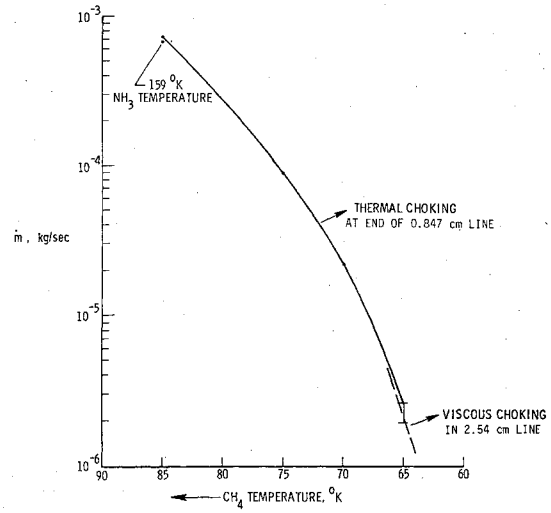

Fig. 6 Gasdynamic-limited mass flow rate.

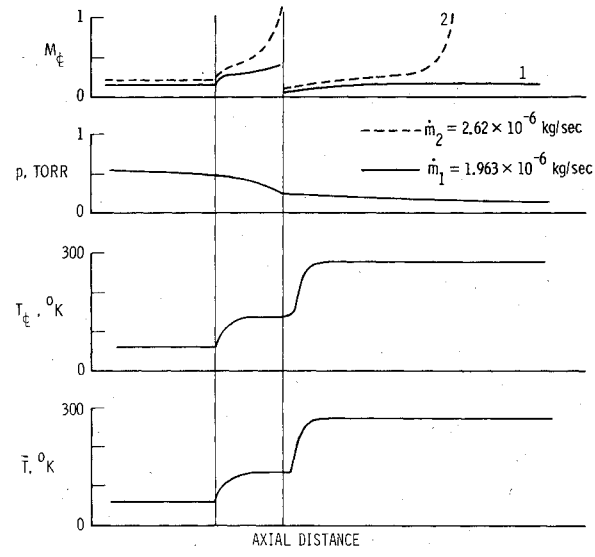

Fig. 7 Gasdynamic results for methane temperature of 65 K.

At the high-temperature end of this scale, the mechanism of a normal shock wave is capable of producing the required initial Mach number. For example, consider the 85 K case: if the Mach number ahead of the shock were 1.55, then the required value of 0.66 on the downstream side could be provided by a normal shock. There is an upper limit to this mechanism, however, since the Mach number downstream of the squib can never exceed about 2.75, even in the absence of friction. A normal shock wave in a Mach 2.75 flow has a Mach number on the downstream side of 0.47. Thus, it appears likely that some mechanism other than normal-shock compression must come into play at the lower methane temperatures. Of course, one of the mechanisms is that very thick boundary layers are present, with large subsonic portions, so that the one-dimensional normal-shock model is quite unrealistic at the lower end of the temperature scale. At this end, friction at the wall becomes a more powerful agent for slowing down the flow.

Nevertheless, it is clear from the trend of the numbers displayed in the table that at some low temperature the model of critical flow at the squib (with a centerline Mach number of one), followed by retardation to a low subsonic Mach number immediately downstream of the squib, is no longer tenable. In this limit, it must be that the compression-wave system propagates upstream of the squib, and calls for a mass flow reduction below the level that corresponds to thermal choking

Table 1 Initial Mach values for $L/D=8$

T, K	$4f_L/D$	$M_{initial}$
65	107.2	0.08
70	9.47	0.25
75	2.60	0.39
85	0.316	0.66

Table 2 Thrust levels

T, K	F, N
65	8.56×10^{-4}
70	9.85×10^{-3}
75	3.59×10^{-2}
85	3.16×10^{-1}

at the end of the 0.847 cm line. Indeed, the computer solution shown as curve 1 of Fig. 7 was already an indication of this occurrence.

Thrust Attributable to the Vent Pipe

Having determined the mass flow rate, it is then a straightforward matter to estimate the thrust due to the flow out of the vent-pipe exit plane. (This thrust is attributed to the vent pipe, and excludes any thrust contributions that might come from subsequent impingement of the exhaust gases on the spacecraft surfaces.) Assuming zero ambient pressure, the one-dimensional formula for the thrust can be written in the form

$$F=\dot{m}V_e[1+(1/\gamma M_e{}^2)]$$

where the velocity V_e and Mach number M_e are averaged over the exit plane. The flow at the exit plane is taken to be frictionally choked, but the actual velocity profile is unknown. The results from the computer solutions discussed earlier show that, at a choked condition, the centerline Mach number usually exceeds one, and drops to low values near the wall. These features are probably also true of the flow at the vent-pipe exit, except that the low ambient pressure may have the effect of thinning the boundary layer, in much the same way that the boundary layer on a hypersonic vehicle is thinned as it approaches the low-pressure region near the base.[9] This tendency to accelerate the layers near the wall is presumably amplified, in the present case, by the occurrence of velocity slip at the wall. Unfortunately, the influences of all these factors are unknown at the present time, although their net effect would be to reduce the momentum flux below the one-dimensional-average value. As a means of approximating this effect, the second term in the equation above is neglected, i.e., the thrust is calculated from $F\approx\dot{m}V_e$ where V_e is taken to be the sonic speed at 280 K, or 436 m/sec. The thrust levels found from this formula are shown in Table 2.

Consistency Checks

The mass flow rates calculated above are consistent with other data from the Nimbus-F flight, namely: the steady-state thrust, the methane tank temperature history, the magnitude of the long-term heat leak, and the cryogen supply lifetime.

Steady-State Thrust

Observations of the rate of change of the orbital period indicate a steady-state thrust level of 15.74 dynes. Using the above thrust formula, this would correspond to a mass flow rate of 3.61×10^{-7} kg/sec. Telemetered data on the tank temperature indicate a methane temperature around 62.5 K. This point is consistent with the values calculated at higher temperatures, which are shown on Fig. 6.

Temperature History

The methane tank temperature can be found from knowledge of the flow rate, if it is assumed that the heat required to cause sublimation of the methane comes from a decrease in the methane temperature. If it is assumed that the thermal diffusivity of the solid methane is large enough to maintain a uniform temperature, then the energy balance gives

$$\dot{m}H_s=mC(\mathrm{d}T/\mathrm{d}t)$$

where H_s is the heat of sublimation, C the heat capacity, and m the mass of the solid methane

$$C=2.3^{+0.08}_{-0.04}\times10^3\ (J/\text{kg-K});$$

$$H_s=6.12\pm0.01\times10^5\ (J/\text{kg})$$

over the temperature range from 63 K to 70 K. A first integral of the heat balance gives

$$m/m_0=\exp[(C/H_s)(T-T_0)]$$

where from the flight data, m_0 was 6.13 kg and the lifetime was 213 days.†† With this relationship, the solution of the heat balance can be written as

$$t-t_0=\frac{m_0C}{H_s}\int_{T_0}^{T}\frac{\exp[(C/H_s)(T-T_0)]}{\dot{m}(T)}\,\mathrm{d}T$$

where the dependence of $\dot{m}$ on T is that given by Fig. 6. This relation was integrated, by Simpson's rule, for initial temperatures of 70, 75, and 85 degrees. The results, shown in Fig. 8, are in reasonable agreement with the flight data. The fact that the observed temperature falls at a slower rate than that predicted may be partly due to imperfect heat transfer, i.e., the calculated $\dot{m}$ assumes that all the energy required for the methane sublimation is immediately available. In fact, the flow of heat from the solid methane itself is limited by its own diffusivity, and by the thermal contact between the cryogen and the tube. A more elaborate calculation would require a coupled solution for this heat-flow problem.

It should also be noted that the initial slope increases sharply with initial temperature; thus the time required to reach the steady-state condition is a weak function of the initial temperature.

Heat Leak

The temperature history derived above assumes that all the required energy comes from a decrease in the internal energy of the methane. However, there is also a heat leak into the methane tank, which affects the temperature. In the steady-state condition, the mass flow rate and heat leak are related by $\dot{Q}=\dot{m}H_s$. The mass flow rate of 3.61×10^{-7} kg/sec calculated above corresponds to a heat leak of 221 mW which appears to be a reasonable value.

Cryogen Lifetime

The mass flow rate reaches the steady-state value in a matter of a day, while the supply lasts for months. Thus, the cryogen lifetime can be estimated from the long-term flow rate of 3.61×10^{-7} kg/sec:

$$t=\frac{6.13\ \text{kg}}{3.61\times10^{-7}\ \text{kg/sec}}=196\ \text{days}$$

which agrees well with the observed lifetime of 213 days. It should be noted that this mass flow was inferred from the

††The authors are grateful to S.H. Siegel of the General Electric Company for providing us with these values.

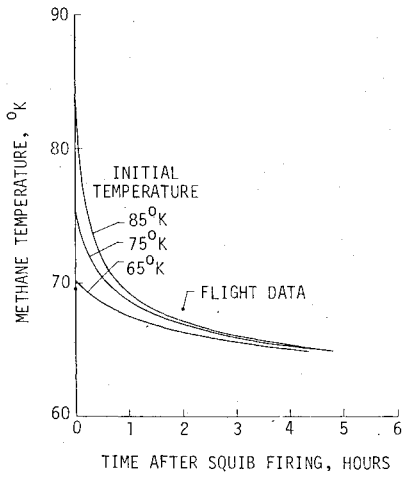

Fig. 8 Methane temperature history, based on gasdynamic-limited mass flow rates.

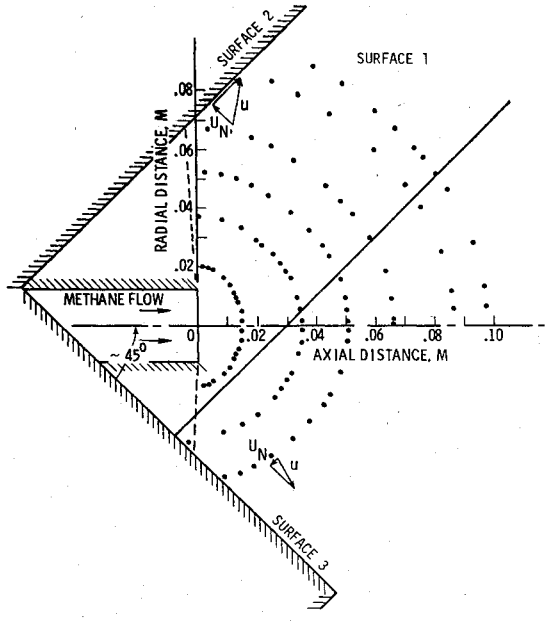

Fig. 9 Plume flowfield for methane at 70 K LRIR configuration. • indicates computation point.

15.74-dyne thrust. If the thrust formula were in error, it would not be possible to recover the cryogen lifetime. The point of these consistency checks is that they all point toward a long-term condition that agrees closely with the calculated mass flow rates.

Results of Plume Flowfield Calculations and Torque Calculations

The machine program described earlier was used to calculate‡‡ the plume flowfield. The input conditions for the plume calculations, i.e., static pressure, static temperature, specific heat ratio, and mass flow rate for each condition of interest were obtained from the internal flow calculations. The flow velocity at the vent-pipe exit was nominally sonic. However, in order to operate the machine program, a Mach number distribution at the exit plane was required. The profile selected was of the form $M(r) = 1 + \epsilon(M_{\ell} - 1)[1 - (r^2/R^2)]$ where $M_{\ell} = 1.2$ and $\epsilon = 0.1$. The results reported herein are not significantly influenced by selection of this profile. The ambient pressure into which the methane expanded was selected to be 1×10^{-3} torr and 1×10^{-6} torr.

‡‡The authors are grateful to J.T. Curtis and J.R. Moselle for performing these calculations.

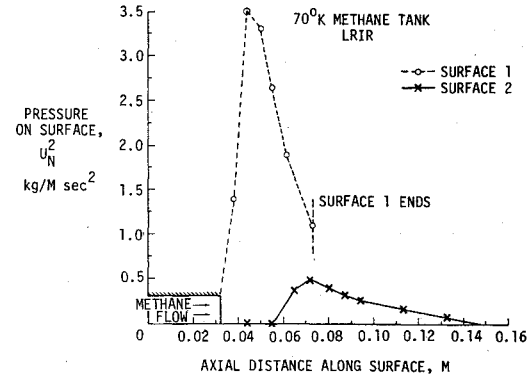

Fig. 10 Axial profile of U_N^2.

Calculations of Impingement Forces

Calculated points at selected values of x and r are shown in Fig. 9 for the plume flowfield associated with the LRIR configuration and a methane temperature of 70 K. The vent pipe is inclined at an angle of approximately 45° relative to surface 3 and is aligned with the spacecraft center of gravity. It can be seen from Fig. 3 that surface 1 is located behind the centerline of the vent pipe as the viewer looks at Fig. 9. At each point of the plume calculation, the computed values of methane density, velocity, local flow angle, and static temperature are printed out. Since these calculations are available as a function of axial and radial coordinates, by properly locating the surfaces of interest in the flowfield relative to the vent pipe it was possible to calculate the distribution of ρu_N^2, where ρ is the local density and u_N is the normal component of velocity, as a function of position on the surfaces. In performing these calculations, it was assumed that when a molecule struck the surface, it gave up all of its normal component of momentum to that surface. The forces caused by particle reflection from one surface to another surface were not included in the calculation.

Figure 10 is typical of the ρu_N^2 results obtained when calculating in the axial direction along surfaces 1 and 2. On the scale of this plot, the ρu_N^2 values on surface 3 were essentially zero because of the very small component of normal velocity at that surface. On the plot shown in Fig. 10, surface 1 results are terminated at about 0.07 m because the edge of the surface has been reached. A similar calculation was performed in order to obtain the ρu_N^2 profile along surface 1 in a direction at 45° to the vent-pipe axis or normal to surface 3.

The plume calculation was also utilized to calculate transverse profiles of ρu_N^2 for each of the surfaces. These results were obtained by calculating at a constant axial location for varying radial distances. The x-coordinate for the surface 1 calculation was near the edge of the LRIR shell and the x-coordinate for the surface 2 radial calculation was approximately 0.075 m. The radial profiles were computed at selected locations on the surfaces and the profiles at the remaining locations were assumed to be similar.

The calculated distributions of ρu_N^2 on surfaces 1 and 2 were hand integrated in order to obtain an estimate of the forces on these surfaces. It can be seen from the results presented that surface 1 experiences the greatest forces because of its proximity to the vent-pipe exit. The integrated force was assumed to act at the approximate location of the peak ρu_N^2 value for the respective surfaces. It was then possible to calculate the x, y, and z moment arms relative to the vehicle center of gravity for each of the surfaces and, therefore, the summation of torques about each of the axes could be calculated. Hand integration of the forces on each of the surfaces represents a relatively crude calculation compared with the sophistication of the gasdynamics calculations performed in order to arrive at the flow conditions in the plume. The mass flow rate calculations are probably accurate to within about 5%. However, for the scope of this investigation, the

Table 3 Summary of LRIR data and impingement calculations – 70 K methane

Torque	Siegel, ACS wheel data, G.E. Nimbus F, LRIR	Calspan calculated values
ΣT_X	$+9.3\times10^{-4}$ N-m	$+10\times10^{-4}$ N-m
ΣT_Y	$+1.5\times10^{-4}$ N-m	$+4\times10^{-4}$ N-m
ΣT_Z	$+8.0\times10^{-4}$ N-m	$+7\times10^{-4}$ N-m

impingement calculation was considered to be a sufficiently accurate approximation.

For the purposes of verifying that plume impingement on nearby surfaces was the source of the torques observed on Nimbus F, the torque values calculated in the manner described earlier were compared with those that were deduced[10] from the Nimbus F attitude control system wheel data. This comparison is illustrated in Table 3. The calculated values are in good agreement with those deduced from flight data, in both magnitude and sign, considering the relatively approximate nature of the impingement calculation. It is reasonable to assume that the calculated torques are accurate to ±25% even though the gasdynamic calculations are considerably more accurate. The good agreement of the calculated and flight data results is most likely due to the fact that the forces on surface 1 are the principal contributor to the observed torques and this surface is relatively easy to work with in summing the forces.

Concluding Remarks

On the basis of the comparison presented in Table 3, it is reasonable to conclude that the torques observed on Nimbus F were probably the result of vent-pipe gas impingement on nearby surfaces and not due to misalignment of the vent-pipe with the vehicle center of gravity. The results do not rule out a small misalignment torque but the impingement calculations do result in the correct signs for each of the torques and approximately the correct magnitudes. Any forces resulting from misalignment would be vector additions to the impingement forces and would still have to result in the correct sign and magnitude of torques.

The results of this study have implications on design practices for open-cycle cryogenic coolers for spacecraft applications. The gases flowing from these devices are subjected to pressure ratios that are effectively infinite, and to thermal environments whose tendency is to raise the stagnation enthalpy of the exhaust gas by a factor of two or greater. Under these circumstances, the effects of compressibility and of thermal or frictional choking play the dominant role in dictating the mass-flow capacities of the system. It is a difficult matter to sort out these coupled effects, especially when they occur at such low Reynolds numbers. The computational techniques used in the present work are a very valuable tool, that can be used to evaluate candidate designs. Future research efforts must address the question of further correlation of these solutions in the compressible regime, so that design charts can be developed for the purpose of homing in more quickly on a satisfactory configuration.

References

[1] Rae, W. J., "Some Numerical Results on Viscous Low-Density Nozzle Flows in the Slender-Channel Approximation," *AIAA Journal*, Vol. 9, May 1971, pp. 811–820.

[2] Rae, W. J., "Final Report on a Study of Low-Density Nozzle Flows with Application to Microthrust Rockets," Calspan Corporation, Buffalo, New York, Report No. AI-2590-A-1, Dec. 1969.

[3] Rothe, D. E., "Electron-Beam Studies of Viscous Flow in Supersonic Nozzles," *AIAA Journal*, Vol. 9, May 1971, pp. 804–811.

[4] Rothe, D. E., "Experimental Study of Viscous Low-Density Nozzle Flows," Calspan Corporation, Buffalo, New York, Report No. AI-2590-A-2.

[5] Curtis, J. T., Moselle, J. R., and Marrone, P. V., "Plume Interference Assessment and Mitigation Program PIAM): Software Deliverable Document," Calspan Corporation, Buffalo, N.Y., Calspan Report No. KC-5305-A-3, Sept. 1973.

[6] Binder, R.C., *Fluid Mechanics*, 2nd Edition. Prentice-Hall, New York, 1949.

[7] Shapiro, A.H., *The Dynamics and Thermodynamics of Compressible Fluid Flow*, Vol. 1, Ronald Press, New York, 1953.

[8] Keenan, J.H. and Kaye, J., *Gas Tables*, Wiley, N.Y., 1948.

[9] Olsson, G.R. and Messiter, A.F., "Hypersonic Laminar Boundary Layer Approaching the Base of a Slender Body," *AIAA Journal*, Vol. 7, July 1969, pp. 1261–1267.

[10] Siegel, S.H., private communication, General Electric Co., Philadelphia, Pa.